Short-Lived α-Emitting Isotope ^{222}Np and the Stability of the $N = 126$ Magic Shell

L. Ma (马龙)[1] Z. Y. Zhang (张志远)[1,2,*] Z. G. Gan (甘再国)[1,2] X. H. Zhou (周小红)[1,2,†] H. B. Yang (杨华彬)[1]
M. H. Huang (黄明辉)[1] C. L. Yang (杨春莉)[1] M. M. Zhang (张明明)[1,2] Y. L. Tian (田玉林)[1] Y. S. Wang (王永生)[1,2,3]
H. B. Zhou (周厚兵)[4] X. T. He (贺晓涛)[5] Y. C. Mao (毛英臣)[6] W. Hua (滑伟)[7] L. M. Duan (段利敏)[1,2]
W. X. Huang (黄文学)[1,2] Z. Liu (刘忠)[1,2] X. X. Xu (徐新星)[1,2] Z. Z. Ren (任中洲)[8]
S. G. Zhou (周善贵)[9,10,11,12] and H. S. Xu (徐瑚珊)[1,2]

[1]*CAS Key Laboratory of High Precision Nuclear Spectroscopy,
Institute of Modern Physics, Chinese Academy of Sciences, Lanzhou 730000, China*
[2]*School of Nuclear Science and Technology, University of Chinese Academy of Sciences, Beijing 100049, China*
[3]*School of Nuclear Science and Technology, Lanzhou University, Lanzhou 730000, China*
[4]*Guangxi Key Laboratory of Nuclear Physics and Technology, Guangxi Normal University, Guilin 541004, China*
[5]*College of Material Science and Technology, Nanjing University of Aeronautics and Astronautics, Nanjing 210016, China*
[6]*Department of Physics, Liaoning Normal University, Dalian 116029, China*
[7]*Sino-French Institute of Nuclear Engineering and Technology, Sun Yat-Sen University, Zhuhai 519082, China*
[8]*School of Physics Science and Engineering, Tongji University, Shanghai 200092, China*
[9]*CAS Key Laboratory of Theoretical Physics, Institute of Theoretical Physics,
Chinese Academy of Sciences, Beijing 100190, China*
[10]*School of Physical Sciences, University of Chinese Academy of Sciences, Beijing 100049, China*
[11]*Center of Theoretical Nuclear Physics, National Laboratory of Heavy Ion Accelerator, Lanzhou 730000, China*
[12]*Synergetic Innovation Center for Quantum Effects and Application, Hunan Normal University, Changsha 410081, China*

A new, very short-lived neutron-deficient isotope ^{222}Np was produced in the complete-fusion reaction ^{187}Re$(^{40}$Ar, 5n$)^{222}$Np, and observed at the gas-filled recoil separator SHANS. The new isotope ^{222}Np was identified by employing a recoil-α correlation measurement, and six α-decay chains were established for it. The decay properties of ^{222}Np with $E_\alpha = 10016(33)$ keV and $T_{1/2} = 380^{+260}_{-110}$ ns were determined experimentally. The α-decay systematics of Np isotopes is improved by adding the new data for ^{222}Np, which validates the $N = 126$ shell effect in Np isotopes. The evolution of the $N = 126$ shell closure is discussed in the neutron-deficient nuclei up to Np within the framework of α-decay reduced width.

Neutron-deficient heavy nuclides, produced as evaporation residues in complete-fusion reactions, decay pervasively by emitting α particles. Therefore, α-decay spectroscopy, one of the oldest yet powerful tools in nuclear physics, has been employed generally to identify new heavy isotopes and to investigate the nuclear structure of ground and excited states in neutron-deficient heavy nuclei [1–4]. As approaching to the proton dripline around $Z = 92$, the synthesis of new isotopes is extremely challenging due to their low production cross sections and short half-lives. In the past few years, we have introduced fast-digital pulse readout electronics and applied it to synthesis of new isotopes based on the gas-filled recoil separator SHANS (spectrometer for heavy atoms and nuclear structure). We carried out a series of experiments aimed at exploring the limit to the existence of uranium and neptunium isotopes and studying the stability of the $N = 126$ shell closure far away from the $Z = 82$ magic number. In these experiments, several new neutron-deficient $Z = 93$ isotopes ^{219,220,223,224}Np [5–8] were observed by using

α-decay spectroscopy, and the α-decay systematics for Np isotopes was extended beyond the proton dripline [5,8]. Our studies suggested that the $N = 126$ magic shell effect would persist in Np isotopes by inspecting the α-decay systematics [8], although a weakening of the $N = 126$ shell stabilization effect towards $Z = 92$ uranium was proposed previously [9]. However, the α-decay systematics is incomplete for Np isotopes due to the lack of experimental information for ^{221,222}Np, and thus it is still an open question how robust the $N = 126$ shell is in Np isotopes.

In this Letter, we report the observation of a new neutron-deficient α-emitting isotope ^{222}Np, which was synthesized in the complete fusion reaction ^{187}Re$(^{40}$Ar, 5n$)^{222}$Np. By combining our experimental findings with the existing data, the convincing evidence for the stability of the $N = 126$ magic shell in Np isotopes is obtained.

The experiment was carried out at the Heavy Ion Research Facility in Lanzhou (HIRFL), China. The ^{40}Ar

ions were accelerated to an energy of 198.7 MeV with a typical intensity of 300 pnA. A ^{187}Re target (enrichment 98.6%) with a thickness of 250 $\mu g/cm^2$ was prepared by sputtering the material onto an 80-$\mu g/cm^2$-thick carbon foil. The beam energy at the center of the target was estimated to be 196.6 MeV using the SRIM program [10], where the maximum cross section of the $5n$ evaporation channel was predicted to occur according to the calculation with the HIVAP code [11].

The gas-filled recoil separator SHANS [12] was used for the separation of recoiled evaporation residues (ERs) from the primary beam particles and the unwanted reaction products. The transport efficiency of the separator was estimated to be 14% by using the test reaction ^{40}Ar + ^{175}Lu. ERs that did not decay in flight through SHANS were implanted into three position-sensitive 16-strip detectors (PSSDs), which were mounted side by side at the focal plane of the separator. Eight side silicon detectors (SSDs) were placed perpendicular to the surface of PSSDs in an open box geometry. They were used to detect the α particles escaping from the PSSDs. The energy, position, and time of the implantation of the ERs and their subsequent α-decay events were measured using these detectors. The total detection efficiency of the detector system for the emitting alpha particles was measured to be 72%. In order to distinguish the α-decay events from the implantation ones, two multiwire proportional counters were mounted upstream from the PSSDs. Behind the PSSDs, three punch-through silicon detectors were positioned for the rejection of signals produced by energetic light particles. Signals from all the preamplifiers of the detection system were recorded by a digital data acquisition system, which consists of 16 waveform digitizers V1724 from CAEN S.p.A [13]. More details of the system were given in Refs. [5,14]. The time of flight of the ^{222}Np ERs through SHANS was estimated to be ~1.2 μs.

Energy calibrations for the PSSDs and SSDs were performed using an external α source and the dominant α-decay peaks from the nuclei produced in the irradiations with ^{175}Lu and ^{186}W targets. The preamplified signals from the PSSDs were recorded in 30-μs-long traces by the waveform digitizers at a 100 MHz sampling frequency [13]. Signals from the same strip with time difference shorter than ~30 μs will pile up and are stored in a single trace. The amplitudes, i.e., energies of signals stored in traces, were extracted by using different types of software algorithms depending on the multiplicity of the recorded signals. For pileup signals, a pulse shape fitting method was used [14], while for single events, a trapezoidal algorithm was adopted [15]. Finally, a typical energy resolution for the PSSDs was obtained to be ~40 keV (FWHM) for 6.5–10 MeV α particles that were registered as single events in the traces, while the reconstructed α lines for the escaping α particles, recorded by the PSSDs and SSDs together, had a poor resolution of about 120–180 keV
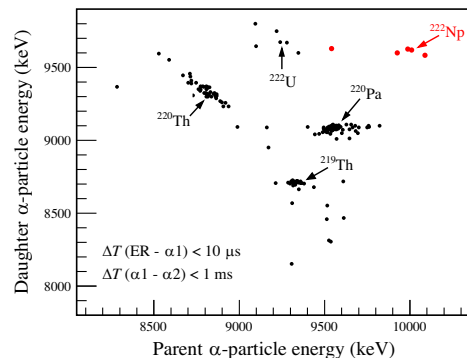

FIG. 1. Two-dimensional scatter plot of parent and daughter α-particle energies for correlated ER-α1-α2 events measured in the PSSDs. Searching times for the ER-α1 and α1-α2 pairs are 10 μs and 1 ms, respectively. The decay events from the new isotope ^{222}Np are labeled by red dots.

(FWHM) for 9.26-MeV α activity. The α-particle energy resolutions associated with pileup events were about 270, 150, 70, and 47 keV for $\Delta T = 100$–200 ns, 200–500 ns, 0.5–1 μs, and $\Delta T > 1$ μs, respectively. Here, ΔT means the time difference between the overlapping signals. For even shorter time difference, $\Delta T < 100$ ns, the α energy deduced from pileup pulses will be rather arbitrary and unreliable.

The identification of rare products of interest was performed by searching the correlated α-decay chains. In the present work, referring to the half-lives of the nuclei close to ^{222}Np and their daughters, the searching time windows were chosen to be 10 μs for ER-α1 pair and 1 ms for the α1-α2 pair. Here, α1 and α2 represent the α particles decaying from the parent (ER) and daughter nuclei, respectively. A two-dimensional scatter plot showing the correlations between the parent and daughter α particles detected in the PSSDs is presented in Fig. 1, which includes all possible pairs of correlated decays whether the third one exists or not. The known $N = 129$ isotones ^{220}Pa and ^{219}Th, having half-lives of around 1 μs, are suitable for examining the ER-α1 pileup trace analysis in the present work. The resolved α-decay energy spectra and the decay curves for ^{220}Pa and ^{219}Th are shown in Fig. 2. The α-decay energies and half-lives measured in the present work are in good agreement with the literature values [16,17]. The correlations originated from known isotopes ^{222}U and ^{220}Th can also be recognized based on the tabulated α-decay properties [9,16]. These nuclei were produced by charged-particle evaporation channels.

The unknown correlations labeled by red dots in Fig. 1, with the parent α-particle energy around 10 MeV and ~9.6 MeV daughter α-particle energy, are assigned to the decay of a new neptunium isotope ^{222}Np, which was produced via the $5n$ evaporation channel. Furthermore, in order to identify the assigned decay chains more reliably, a full ER-α-α-α correlation analysis was conducted
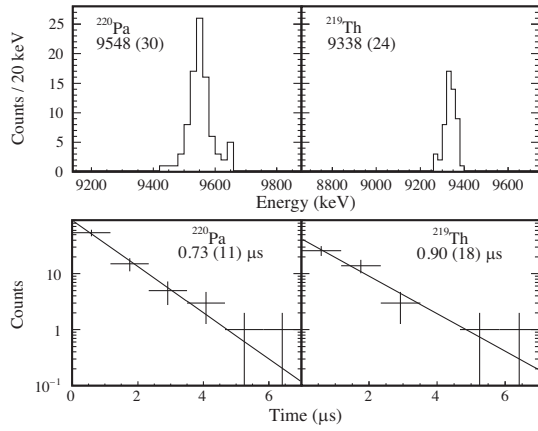
FIG. 2. Energy spectra and decay curves of α particles emitted from ^{220}Pa and ^{219}Th. The data were obtained by using a pulse shape fitting method given in Ref. [14].

requiring that both the ER-like and the α-like events occurred within 40 s in the same position of the stop detectors. Finally, six correlated α-decay chains were established for ^{222}Np and their details are displayed in Fig. 3. For chain 6 shown in Fig. 3, the α particle decaying from ^{218}Pa was not observed. It is noted that, due to the specific searching time intervals applied, only the $\alpha1$-$\alpha2$ correlations from chains 1–5 with full-energy α-decay events are visible in Fig. 1. Two traces, corresponding to chains 1 and 5, are presented in Fig. 4 as examples to show the ER-$\alpha1$ pileup pulses where ^{222}Np was registered.

From chains 2–6, a mean energy of 10 016(33) keV was deduced for the α decay of ^{222}Np. Here, it should be noted that the parent α-particle energy in chain 1 was not used for the extraction, because of a much worse energy resolution due to the extremely short time interval between the implantation and the subsequent α decay. An α-decay half-life of $T_{1/2} = 380^{+260}_{-110}$ ns was deduced for ^{222}Np by averaging the time differences between ^{222}Np implantations and decays. From chains 1–5, a half-life of $T_{1/2} = 127^{+102}_{-39}$

μs and an energy of 9602(17) keV were determined for the α decay of ^{218}Pa, which agrees well with the literature data [16,18]. Similarly, a half-life of $T_{1/2} = 11.5^{+7.9}_{-3.3}$ s and an energy of 7223(17) keV were derived for the α decay of ^{214}Ac, in good agreement with the literature values [16]. The error bars of the half-lives in the present work were determined by the maximum likelihood method described in Ref. [19].

The presence of the $N = 126$ shell closure above the doubly magic nuclide ^{208}Pb has been studied extensively by inspecting the α-decay systematics. Along an isotopic chain, when crossing the $N = 126$ shell closure, the largest α-decay energy and consequently shortest half-life are expected to occur for the nuclide with $N = 128$, which decay to a daughter with $N = 126$ magic number. The α-decay Q_α values and partial half-lives $T^\alpha_{1/2}$ for presently known neutron-deficient $89 \leq Z \leq 93$ isotopes are shown in Fig. 5. For ^{222}Np, a 100% branching ratio was assumed for the calculation of $T^\alpha_{1/2}$. From Fig. 5, we can see that the new α-decay properties of ^{222}Np fit well into the Q_α and $T^\alpha_{1/2}$ systematics of the Np isotopes. The improved systematics of α-decay properties for the Np isotopes indicates strongly that the unknown ^{221}Np ($N = 128$) would have the largest Q_α values and shortest $T^\alpha_{1/2}$ along the Np isotopic chain. In order to complete the α-decay systematics, it is desirable to synthesize the $N = 128$ isotope ^{221}Np. In our previous work, the isotope ^{220}Np was synthesized by employing the ^{40}Ar + ^{185}Re reaction [8], in which ^{221}Np would have a comparable yield as that of ^{220}Np according to the HIVAP calculation. However, we did not observe any decay events of ^{221}Np, while eight α-decay chains were built for ^{220}Np. As suggested by the α-decay systematics, the half-life for ^{221}Np might be only several tens of ns, too short to survive the flight through the separator.

The experimental data are also compared with selected theoretical models in Fig. 5. The theoretically predicted Q_α values in Ref. [22] were presented in Fig. 5(a). In Ref. [22], a number of simple Q_α relations for four neighboring nuclei
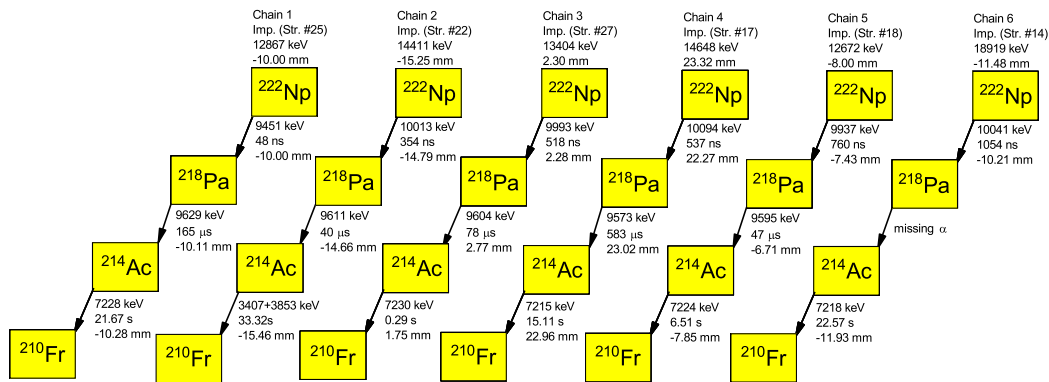

FIG. 3. Correlated α-decay chains of ^{222}Np in the present work. Each chain is labeled with an identification number, strip number of PSSDs, implantation energy of ER events, decay energies, time intervals, and vertical positions. All the events in each chain were observed within a position window of ±2.0 mm for full energy deposited in the PSSDs. Case marked "missing α" denotes an event with no-energy collected in the implantation PSSDs.
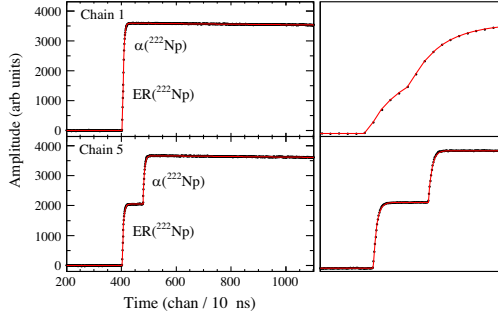
FIG. 4. Examples of traces where ^{222}Np was registered (dotted lines). The red solid lines are the fitted curves based on the method in Ref. [14]. Right panel: enlarged traces for the rising edge region.

were constructed in terms of the longitudinal Garvey-Kelson relation [25] and the odd-even features [26]. The measured decay energy Q_α of ^{222}Np [10.200(33) MeV] was reproduced very well by the predicted 10.141-MeV value [22]. The partial α-decay half-lives $T^\alpha_{1/2}$ of the Ac-Np isotopes were calculated from the experimental Q_α values according to a new Geiger-Nuttall law proposed by Ren *et al.* [23,24], which were presented in Fig. 5(b).
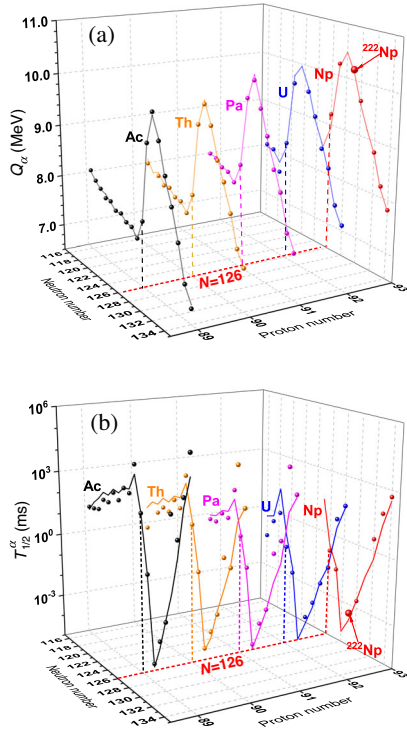

FIG. 5. (a) Systematics of α-decay Q_α values and (b) α-decay half-lives $T^\alpha_{1/2}$ of the g.s. to g.s. transitions for neutron-deficient $89 \leq Z \leq 93$ isotopes as a function of proton number and neutron number. The solid spheres refer to literature values taken from Refs. [5,6,8,9,16,20,21]. The red bigger solid spheres represent the results measured in the present work. The solid lines refer to the theoretical predictions taken from Refs. [22–24].

We can find a nice agreement between the predicted half-lives and the experimental values for Np isotopes.

In order to gain a further insight into the evolution of the $N = 126$ shell closure in Np ($Z = 93$) isotopes, one can study the trend of the reduced widths (δ^2) at variance of neutron number. The δ^2 values can be extracted from the α-decay energies and partial half-lives according to the prescription proposed by Rasmussen [27]. The new α-decay data on ^{222}Np and our previous data on ^{219,220,223}Np [5,6,8] allow us to extend the trends of δ^2 in the $N = 126, 127, 129,$ and 130 isotones up to Np. The systematics of δ^2 values for the $N = 126$–130 isotones from Po through Np is shown in Fig. 6, which was constructed combining our data with literature values for Po-U [9,16,20,28,29]. The previous work suggested that the valance proton in the ground state of odd-Z neutron-deficient At-Np nuclei occupies dominantly the $h_{9/2}$ orbital [6,30], and consequently we use $\Delta l = 0$ for all even-N Po-Np isotopes. Here Δl denotes the angular momentum of the emitted α particle. In the case of the $N = 129$ isotones, we also employ $\Delta l = 0$ since only decays populating the same states in the daughter nuclei were taken [9,16,17,30]. For the $N = 127$ isotones, the $\Delta l = 5$ was assumed for the decays proceeding from the initial $\nu(2g_{9/2})^1$ to the final $\nu(3p_{1/2})^{-1}$ orbital [9,31,32]. As shown in Fig. 6, the δ^2 values of the $N = 128, 129,$ and 130 isotones are apparently larger than those of the $N = 126$ and 127 isotones up to Pa ($Z = 91$), clearly indicating a strong effect of the $N = 126$ shell closure. It is worth noting that the δ^2 values of ^{218}U ($N = 126$) and ^{222}U ($N = 130$) get much closer, possibly implying a weakening of the $N = 126$ shell stabilization effect for U [9]. The δ^2 values of the Np
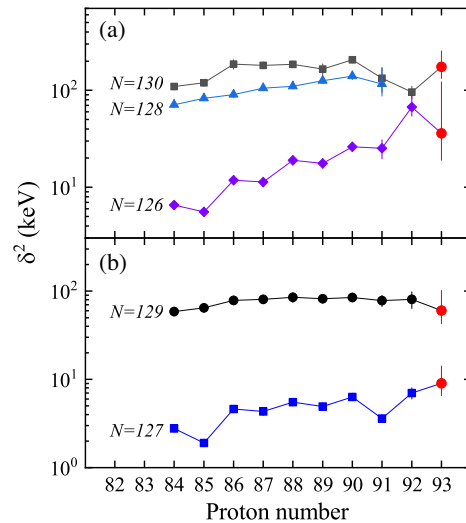

FIG. 6. Reduced α-decay widths δ^2 of even-N (a) and odd-N (b) Po-Np isotopes as a function of proton number. The reduced widths of ^{219}Pa, ^{219}U, and ^{215}At were deduced from the latest data [6,28,29]. The red dots represent the values of Np isotopes deduced from Refs. [5,6,8] and this Letter.

isotopes are presented with red points in Fig. 6, of which the δ^2 value of the ^{219}Np ($N = 126$) has a big error. Generally, the δ^2 value for each of the Np nuclides follows the trend of its corresponding lighter isotones except the U ($N = 126$ and 130) isotopes. The sudden increase of δ^2 values when across the $N = 126$ magic shell seems still present at $Z = 93$. Regardless of the large uncertainty associated with ^{219}Np, the behavior of the δ^2 values might indicate the persistence of the $N = 126$ shell closure in Np isotopes.

In summary, we have reported the discovery of the $N = 129$ isotope ^{222}Np, which was produced in the fusion evaporation reaction ^{40}Ar + ^{187}Re. With the digital electronics and the energy-position-time correlation measurement, the α-particle energy and half-life of ^{222}Np were determined to be $E_\alpha = 10016(33)$ keV and $T_{1/2} = 380^{+260}_{-110}$ ns, respectively. By inspecting the systematics of the α-decay Q_α values, half-lives, and reduced α-decay widths, the persistent rigidity of the $N = 126$ magic number in Np isotopes is clearly recognized in the present study. The future experiments will aim at synthesizing the heavier neutron-deficient Pu and Am isotopes to further explore the evolution of the $N = 126$ shell closure beyond $Z = 92$.

---

*Corresponding author.
zhangzy@impcas.ac.cn
†Corresponding author.
zxh@impcas.ac.cn

[1] A. N. Andreyev, M. Huyse, P. Van Duppen, C. Qi, R. J. Liotta *et al.*, Phys. Rev. Lett. **110**, 242502 (2013).

[2] Z. Kalaninova, S. Antalic, A. N. Andreyev, F. P. Hessberger, D. Ackermann *et al.*, Phys. Rev. C **89**, 054312 (2014).

[3] H. De Witte, A. N. Andreyev, S. Dean *et al.*, Eur. Phys. J. A **23**, 243 (2005).

[4] J. Uusitalo, S. Eeckhaudt, T. Enqvist *et al.*, Eur. Phys. J. A **25**, 179 (2005).

[5] H. B. Yang, L. Ma, Z. Y. Zhang *et al.*, Phys. Lett. B **777**, 212 (2018).

[6] M. D. Sun, Z. Liu, T. H. Huang *et al.*, Phys. Lett. B **771**, 303 (2017).

[7] T. H. Huang, W. Q. Zhang, M. D. Sun, Z. Liu, J. G. Wang *et al.*, Phys. Rev. C **98**, 044302 (2018).

[8] Z. Y. Zhang, Z. G. Gan, H. B. Yang, L. Ma, M. H. Huang *et al.*, Phys. Rev. Lett. **122**, 192503 (2019).

[9] J. Khuyagbaatar, A. Yakushev, Ch. E. Düllmann, D. Ackermann, L. L. Andersson *et al.*, Phys. Rev. Lett. **115**, 242502 (2015).

[10] J. F. Ziegler, M. D. Ziegler, and J. P. Biersack, Nucl. Instrum. Methods Phys. Res., Sect. B **268**, 1818 (2010),

[11] W. Reisdorf, Z. Phys. A **300**, 227 (1981).

[12] Z. Y. Zhang, L. Ma, Z. G. Gan *et al.*, Nucl. Instrum. Methods Phys. Res., Sect. B **317**, 315 (2013).

[13] V1724 & VX1724 User Manual, http://www.caen.it/csite, 2018.

[14] H. B. Yang, Z. G. Gan, Z. Y. Zhang, M. M. Zhang, M. H. Huang, L. Ma, and C. L. Yang, Eur. Phys. J. A **55**, 8 (2019).

[15] V. T. Jordanov and G. F. Knoll, Nucl. Instrum. Methods Phys. Res., Sect. A **345**, 337 (1994).

[16] NNDC National Nuclear Data Center, Chart of Nuclides, https://www.nndc.bnl.gov/nudat2.

[17] T. H. Huang, W. Q. Zhang, M. D. Sun, Z. Liu, J. G. Wang *et al.*, Phys. Rev. C **96**, 014324 (2017).

[18] F. P. Heßberger, S. Hofmann, D. Ackermann, V. Ninov, M. Leino, S. Saro, A. Andreyev, A. Lavrentev, A. G. Popeko, and A. V. Yeremin, Eur. Phys. J. A **8**, 521 (2000).

[19] K.-H. Schmidt, C.-C. Sahm, K. Pielenz, and H.-G. Clerc, Z. Phys. A **316**, 19 (1984).

[20] A. P. Leppanen, J. Uusitalo, M. Leino, S. Eeckhaudt, T. Grahn *et al.*, Phys. Rev. C **75**, 054307 (2007).

[21] L. Ma, Z. Y. Zhang, Z. G. Gan, H. B. Yang, L. Yu *et al.*, Phys. Rev. C **91**, 051302(R) (2015).

[22] M. Bao, Z. He, Y. M. Zhao, and A. Arima, Phys. Rev. C **90**, 024314 (2014).

[23] Y. Ren and Z. Ren, Phys. Rev. C **85**, 044608 (2012).

[24] Y. Ren and Z. Ren, Nucl. Sci. Tech. **24**, 050518 (2013), http://www.j.sinap.ac.cn/nst/EN/Y2013/V24/I5/50518.

[25] G. T. Garvey, W. J. Gerace, R. L. Jaffe, I. Talmi, and I. Kelson, Rev. Mod. Phys. **41**, S1 (1969).

[26] Y. Y. Cheng, Y. M. Zhao, and A. Arima, Phys. Rev. C **89**, 061304(R) (2014).

[27] J. O. Rasmussen, Phys. Rev. **113**, 1593 (1959).

[28] A. Samark-Roth, L. G. Sarmiento, D. Rudolph, J. Ljungberg, B. G. Carlsson *et al.* Phys. Rev. C **98**, 044307 (2018).

[29] M. M. Zhang, Y. L. Tian, Y. S. Wang, X. H. Zhou, Z. Y. Zhang *et al.* Phys. Rev. C **100**, 064317 (2019).

[30] E. Caurier, M. Rejmund, and H. Grawe, Phys. Rev. C **67**, 054310 (2003).

[31] C. Xu and Z. Ren, Phys. Rev. C **76**, 027303 (2007).

[32] Y. Qian and Z. Ren, Nucl. Phys. **A852**, 82 (2011).